The paper was published in the proceedings of the 11th International Conference on Physical Modelling in Geotechnics (ICPMG2026) and was edited by Ioannis Anastasopoulos. The conference was held from June 8th to June 12th 2026 in Zurich, Switzerland.

Centrifuge model tests of cantilever pile supported foundation pit

Xiaomeng Xue, Ga Zhang
Tsinghua University, Beijing, China, xxm23@mails.tsinghua.edu.cn, zhangga@tsinghua.edu.cn

ABSTRACT: The rapid advancement of urbanization has led to a growing prevalence of large-scale foundation pits. As a retaining structure with simple geometry and convenient construction, cantilever piles are extensively utilized in various supporting systems. In order to simplify the calculation model in numerical simulation, the cantilever pile is usually equated to diaphragm wall using equivalent stiffness method. However, this method cannot reasonably consider the pile-soil interaction. Three centrifuge model tests were conducted to investigate the effects of pile length and pile spacing on the stress and deformation characteristics of the structure and failure response of the soil. The results show that increasing the pile length and decreasing the pile spacing could reduce the deformation of the supporting piles and the soil, but the displacement distribution pattern was maintained. The reduction of pile spacing was more significant for the deformation control of the foundation pit than pile length. The maximum values of bending moment of the supporting piles were located above the excavation surface, and the position of the maximum axial force was at the bottom of the pile. Both the longer supporting piles and the smaller pile spacing reduced the bending moment and axial force. The retained soil cracked at a distance of 0.4-0.6 times pile length from the supporting piles, and the deformation localization occurred there. The supporting effect was improved by reducing the deformation localization.

1 INTRODUCTION

The accelerated development of urbanization leads to more and more utilization of underground space. The underground engineering inevitably requires foundation pit excavation (Hu et al., 2024), and supporting measures (such as the cantilever system and the internal bracing system) are adopted to reduce the impact of excavation on the surrounding soil (Liu et al., 2023). Therefore, the response prediction of the supporting structure and the nearby environment after excavation is pivotal. Currently, the main research methods include four categories: physical tests, numerical simulations, field observations and analytical methods (Zhang et al., 2021; Li et al., 2025; Ren et al., 2023; Wang et al., 2023). Numerical simulation is widely used in stress and deformation calculations during the excavation because of its efficiency and accuracy. The most common simulation method is the finite element or finite difference model based on commercial software (Liu et al., 2020). The supporting piles were normally equated to the diaphragm wall through the equivalent stiffness method to simplify the calculation model. Specifically, the thickness of the diaphragm wall was determined by equating the bending stiffness of the supporting piles to that of the diaphragm wall. However, this method ignored the interaction between the piles and the soil, leading to the large discrepancy of the calculation results with the actual data.

The deformation modes and failure characteristics of narrow foundation pits with various width-to-height ratios supported by cantilever piles were studied through model tests (Hu et al., 2024). The double-layer pile-supported structure could effectively inhibit soil slippage and minimize crack formation between piles. (Chi et al., 2024). The numerical methods were used to establish an orthogonal test calculation model to analyze the behavior of foundation pits with different pile length and pile spacing, and obtained the significant factor in evaluating the settlement control effect (Song et al., 2025).

In this paper, a series of centrifuge model tests of foundation pits supported by cantilever piles with different pile spacings and embedded depths were conducted to study the force and deformation characteristics of the supporting piles and the displacement response of the soil. The main contents are as follows: (1) to observe the deformation distribution law of supporting piles and soil after excavation; (2) to analyze the mechanical properties of supporting piles during excavation; (3) to analyze the pile-soil interaction and reinforcement mechanism of supporting piles.

2 TEST

2.1 Device and measurement

The centrifuge model tests were performed using the geotechnical centrifuge at Tsinghua University, which has a maximum acceleration capacity of 250 g and an effective radius of 2 m. The model container dimension is 600 mm in length, 200 mm in width, and 550 mm in height. A 40-mm-thick transparent plexiglass was installed on the long side of the container to observe the deformation of the foundation pit during testing. The plexiglass was coated with lubricant to minimize boundary effects. As shown in Figure 1, a customized excavation device was installed on the model container to simulate the true paths of the stress and deformation in-flight of the foundation pit (Zhang and Yan 2016).

During the centrifuge model tests, an image capture system recorded the model deformation as a series of images. The displacement field of the model was then quantitatively analyzed using an image-based measurement system (Zhang et al., 2009), which employed the correlation-based algorithm of image sequence. In addition, seven pairs of strain gauges were attached along the center axis of the supporting pile to record the strain history during the tests, and the location of the strain gauges was shown in Figure 2. The bending moment of the supporting pile could be obtained from the measured strain according to the elasticity theory.

In this paper, all results are transformed to prototype size according to the similarity law at the 50 g level. The length and displacement of the model are 1/50 of the prototype, the bending moment is $1/50^3$ of the prototype, the axial force is $1/50^2$ of the prototype, the bending stiffness is $1/50^4$ of the prototype, the stress and strain are equal to the prototype. A Cartesian coordinate system was established with the midpoint of the pile top as the origin point. The positive directions were stipulated as rightwards of x-axis and downwards of z-axis as shown in Figure 2.

2.2 Model and schemes

The model was made of cohesive soil with a dry density of 1.65 g/cm^3 and an initial water content of 17%. The specific gravity of the soil was 2.7. The plastic limit and liquid limit of the soil were 18.5% and 25%, respectively. The soil was prepared using layer-wise compaction method. White particles were randomly distributed on the observation side of the soil to improve the accuracy of test results.

The test models were designed based on practical engineering and experimental equipment. The soil base was 600 mm in length, 200 mm in width, and 450 mm in height and the excavated soil was 300 mm in length, 200 mm in width, and 150 mm in height (Figure 2). In the prototype scale, the foundation pit was 30 m in length, 10 m in width, and 22.5 m in height, with an excavation length of 15 m and a depth of 7.5 m. The supporting piles were made of aluminum alloy with a 15 mm×15 mm (prototype: 750 mm×750 mm) square cross-section. Piles were inserted vertically into the soil in a row. Three centrifuge model tests were conducted to study the deformation behavior and mechanical characteristics with various pile spacings and lengths during excavation. The specific setup of the tests is shown in Table 1, with all dimensions scaled to the prototype.

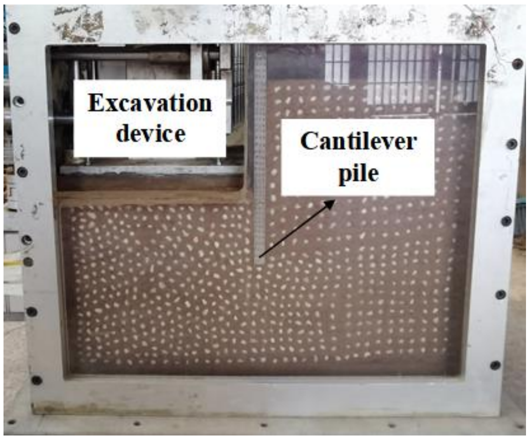

Figure 1. Schematic view of test model.

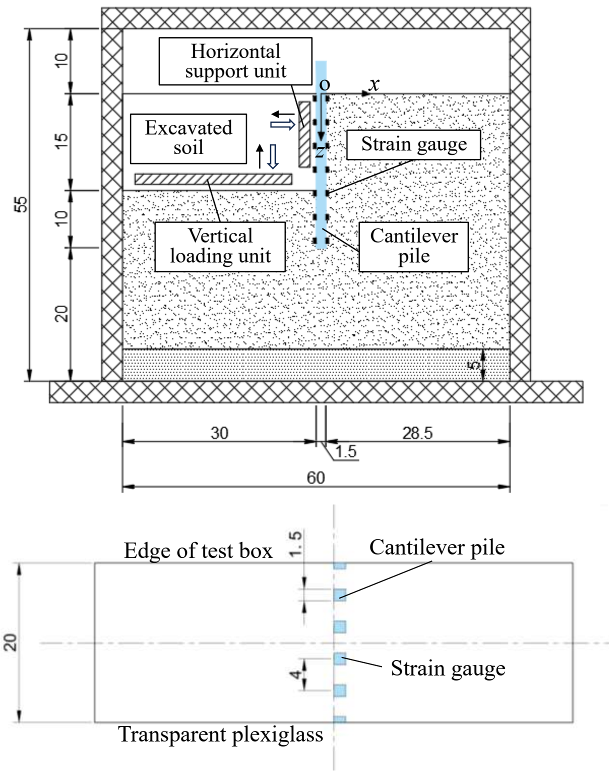

Figure 2. Schematic view of layouts of piles and strain gauge (unit:cm).

Table 1. Centrifuge model test program.

Test	#1	#2	#3
pile quantity	9	6	6
pile spacing (m)	1.44	2	2
pile length (m)	12.5	12.5	15
excavation depth (m)	7.5	7.5	7.5
embedded depth (m)	5	5	7.5

2.3 Procedure

Considering both the actual construction sequence and centrifuge operation requirements, the model testing procedure was designed as follows:

Step 1: Consolidation of the soil base. The soil base was prepared through layered compaction in the model container. After securing the container to the centrifuge basket, the centrifugal acceleration was gradually increased from 1 g to 50 g in 10 g increments. Each acceleration level was maintained until soil deformation stabilized.

Step 2: Excavation of the foundation pit. After the soil deformation was stabilized at 50 g, the commands were sent to the excavation device through a control circuit connected to the centrifuge control switch, and the soil excavation was completed under 50 g. Then the centrifugal acceleration was retained at 50 g until the deformation of the model stabilized.

3 RESPONSE OF SUPPORTING PILE

3.1 Displacement response

Figure 3 presents the histories of horizontal displacement at the tops of the supporting piles with various pile lengths and pile spacings. Among the three tests, the horizontal displacement at the top of the pile of Test #2 (pile spacing 2 m, pile length 12.5 m) was maximum, and that of Test #1 (pile spacing 1.44 m, pile length 12.5 m) was minimum. The results indicated that the pile spacing was more effective in limiting the horizontal displacement at the top of the pile than pile length. The development law of the horizontal displacement with time in the three tests was similar. The displacement increased rapidly at the early stage and gradually slowed down with time increasing until stabilized.

Figure 4 shows the vertical distributions of the horizontal displacement of the supporting piles. The supporting piles demonstrated a global deflection toward the excavated side. The maximum horizontal displacement occurred at the pile top and decreasing linearly with increasing elevation, and a slight displacement toward the retained side was observed at the pile bottom. The deformation mode of the supporting pile was hardly affected by the pile length and pile spacing.

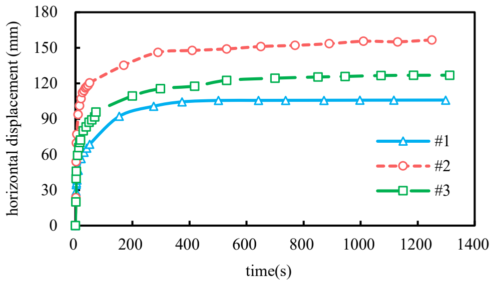

Figure 3. Histories of horizontal displacement at the tops of the supporting piles with various pile lengths and pile spacings.

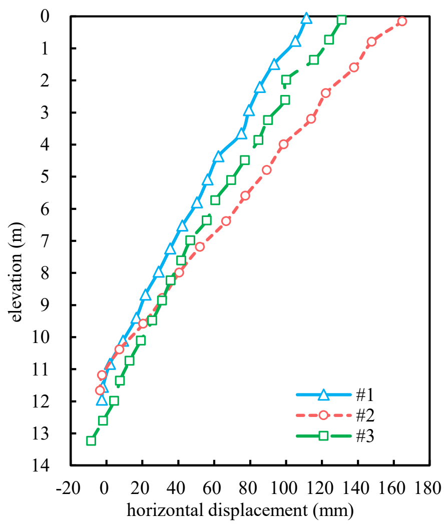

Figure 4. Vertical distributions of the horizontal displacement of the supporting piles.

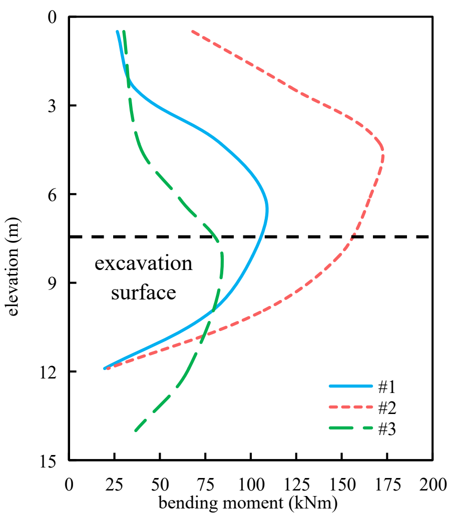

Figure 5. Bending moment distributions of the supporting piles with various pile lengths and pile spacings.

3.2 Stress analysis

Figure 5 compares the bending moment distributions of the supporting piles with various pile lengths and pile spacings. The bending moment was calculated from strain gauge measurements using elastic beam theory. It can be seen that all curves exhibited an approximately parabolic distribution with a peak, and the location of the peak occurred above the excavation surface. The maximum bending moment of Test #2 (pile spacing 2 m, pile length 12.5 m) was greatest while that of Test #3 (pile spacing 2 m, pile length 15 m) was smallest. The results indicated that the bending moment of the pile reduced with increasing pile length and decreasing pile spacing. However, the distribution pattern of the bending moment maintained constant with different pile lengths and pile spacings.

Figure 6 compares the axial force distributions of the supporting piles with various pile lengths and pile spacings. The entire supporting pile was under pressure, and the axial force was larger at both ends of the supporting pile and smaller in the middle. The maximum axial force occurred in Test #2 (pile spacing 2 m, pile length 12.5 m), while the minimum was observed in Test #1 (pile spacing 1.44 m, pile length 12.5 m). Both longer pile length and smaller pile spacing could reduce the axial force of the supporting pile.

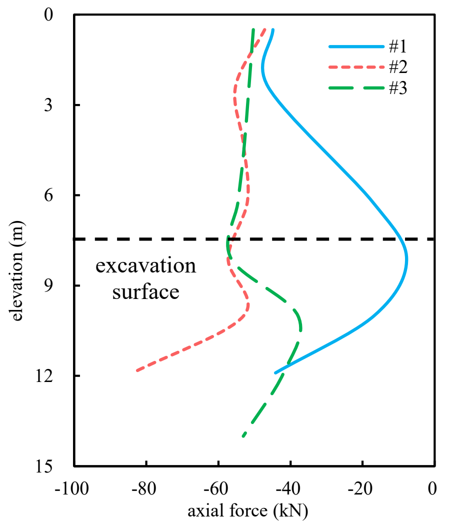

Figure 6. Axial force distributions of the supporting piles with various pile lengths and pile spacings.

4 RESPONSE OF SOIL

4.1 Displacement of the retained soil

Figure 7 shows the horizontal distributions of horizontal displacement and vertical displacement of retained soil surface with various pile lengths and pile spacings. It can be seen that both the increased pile length and decreased pile spacing could reduce the deformation of the retained soil, and the pile spacing demonstrated a more pronounced controlling effect on the soil deformation. The horizontal displacement decreased as the horizontal distance from the supporting pile increased. A sudden decrease of the horizontal displacement occurred at a distance of approximately 0.5 times pile length from the supporting pile, and significant crack was observed in the model soil. The distribution pattern of horizontal displacements and the location of the mutation point was basically the same for the three tests. The deformation of the retained soil could be divided into the main influence zone and the fringe influence zone based on the mutation point. The settlement of the retained soil progressively decreased with the increasing horizontal distance from the supporting pile. Different from the horizontal displacement, the settlement distribution was continuous with no mutation point.

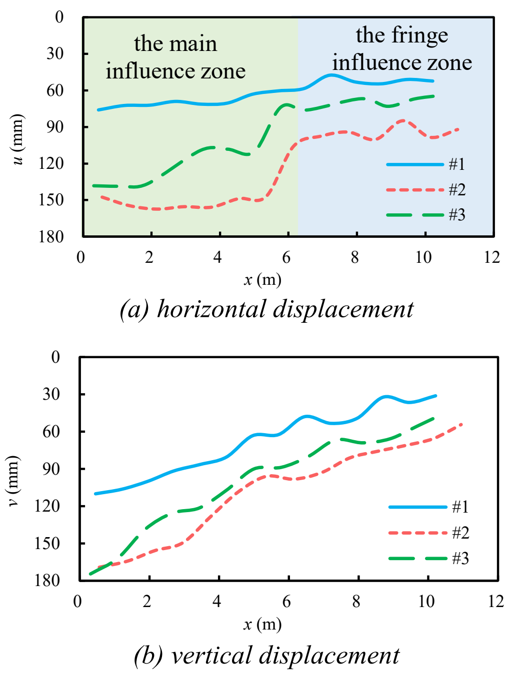

Figure 7. Horizontal distributions of displacements of retained soil surface with various pile lengths and pile spacings.

4.2 Basal heave

Figure 8 shows the horizontal distributions of horizontal displacement and vertical displacement of soil surface at the excavated side with various pile lengths and pile spacings. The soil deformation of Test

#1 (pile spacing 1.44 m, pile length 12.5 m) was smallest, and that of Test #2 (pile spacing 2 m, pile length 12.5 m) and Test #3 (pile spacing 2 m, pile length 15 m) were essentially equal. The effect of pile length was imperceptible on restricting the soil deformation at the excavated side. The horizontal displacement of the soil was towards the excavated side and decreased with the increasing distance from the supporting pile. The influence range of horizontal displacement was approximately within 4 m from the supporting pile. The basal heave of the soil initially increased and then decreased, the maximum heave occurred at approximately 1.5 m from the supporting pile, and the locations of peak heave were remained constant with various pile lengths and pile spacings.

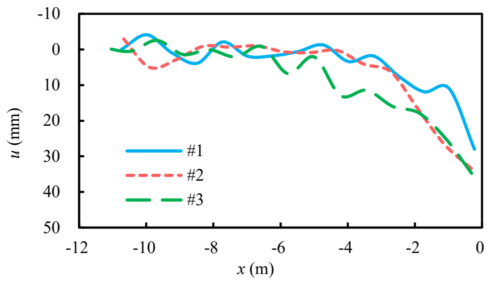

(a) horizontal displacement

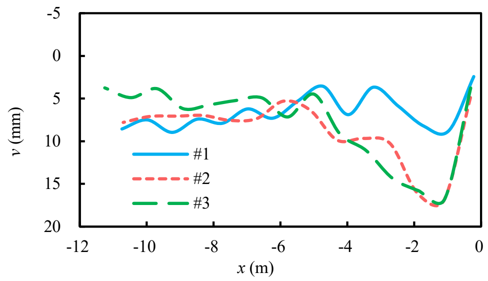

(b) vertical displacement

Figure 8. Horizontal distributions of displacements of soil surface at the excavated side with various pile lengths and pile spacings.

5 PILE REINFORCEMENT MECHANISM

5.1 Failure mechanism

Figure 9 presents the horizontal distributions of horizontal strain of the retained soil at various elevations. A four-node isoparametric square elements (10 mm side length) were used for strain computation based on the finite element method, with the node displacements directly measured by the image analysis. The sign convention defined tensile strain as positive and compressive strain as negative. It can be seen that the horizontal strain of the retained soil decreased with increasing elevations. The horizontal strain peaked at the soil surface in an area of 0.4-0.6 times pile length from the supporting pile, while otherwise the horizontal strain remained small. The deformation was concentrated within this area, namely the deformation localization appeared there. And the crack of soil was observed at this location, demonstrating that the deformation localization has triggered localized failure.

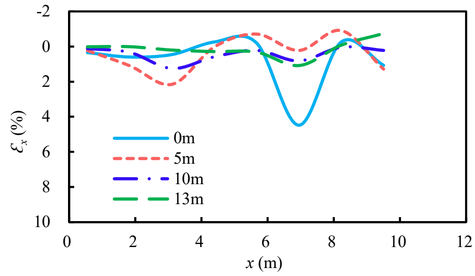

(a) *Test#1*

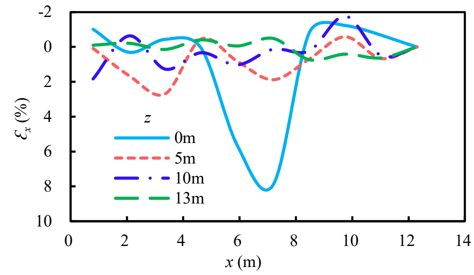

(b) *Test#2*

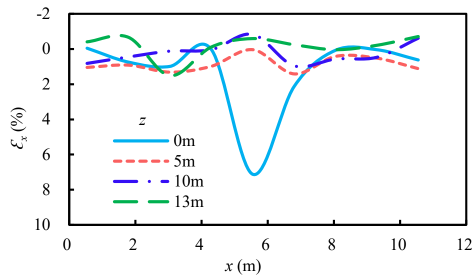

(c) *Test#3*

Figure 9. Horizontal distributions of horizontal strain of the retained soil at various elevations.

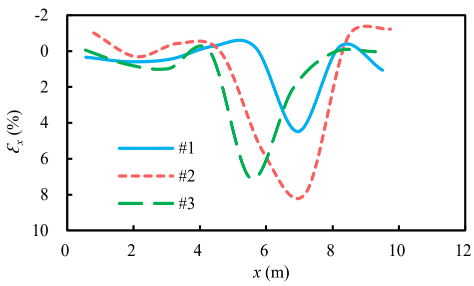

Figure 10. Horizontal strain distributions of the retained soil surface with various pile lengths and pile spacings.

Figure 10 compares the horizontal strain distributions of the retained soil surface with various pile lengths and pile spacings. The peak horizontal strain was greatest in Test #2 (pile spacing 2 m, pile length 12.5 m), followed by Test #3 (pile spacing 2 m, pile length 15 m), and that in Test #1 (pile spacing 1.44 m, pile length 12.5 m) was smallest. Both the increased pile length and the decreased pile spacing could reduce the peak horizontal strain of the retained soil, thereby the deformation localization of the soil was reduced. Compared with pile length, smaller pile spacing demonstrated greater efficacy in reducing soil deformation localization, resulting in superior reinforcement performance.

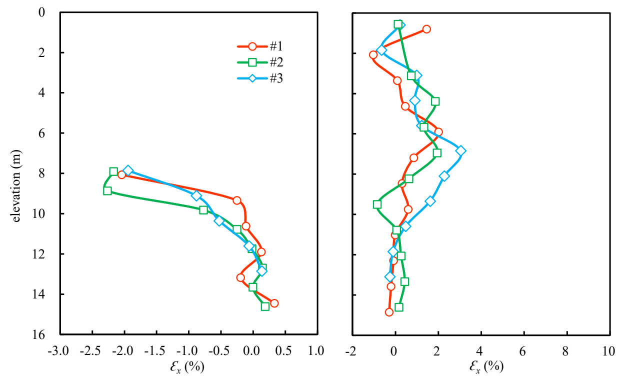

(a) *1 m from the supporting pile*

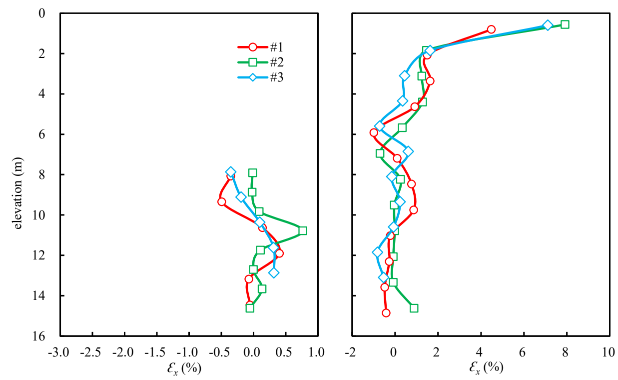

(b) *5 m from the supporting pile*

Figure 11. Vertical distributions of horizontal strain of the soil at different horizontal distances from the piles.

5.2 Pile-soil interaction

Figure 11 shows the vertical distributions of horizontal strain of the soil at different horizontal distance from the supporting piles. The soil was compressed on the excavated side and was tensioned on the retained side, which was closely correlated to the deformation mode of the supporting pile. At a distance of 1 m behind the supporting pile, the maximum horizontal strain of the retained soil occurred at a depth of approximately half the pile length. In contrast, at a distance of 5 m behind the pile, the maximum horizontal strain was observed near the soil surface. The location of strain localization was progressively towards the supporting pile with increasing depth. The results indicated that there was a potential slip surface in the retained soil, with the sliding body exhibited an approximately triangular-shaped configuration.

6 CONCLUSIONS

Through the centrifuge model tests of the foundation pit supported by cantilever piles with various pile lengths and pile spacings under excavation condition, the following conclusions can be drawn:

(1) Both increasing the pile length and decreasing the pile spacing could reduce the deformation of the supporting piles and the soil, and the pile spacing was a more important factor to control the deformation of the foundation pit.

(2) The bending moment and the axial force of the supporting pile decreased with increasing pile length and decreasing pile spacing. The maximum bending moments were consistently located above the excavation surface.

(3) Deformation localization of the retained soil occurred in the range of 0.4-0.6 times pile length from the supporting pile, leading to the development of tensile cracks. The cantilever piles were used to reinforce foundation pits by limiting the development of deformation localization of the soil.

(4) The deformation of the supporting pile induced tensile strain in the retained soil and compressive strain in the soil at the excavated side. The maximum horizontal strain in the retained soil occurred at progressively shallower depths as the distance from the pile increased, with a concurrent growth in magnitude. The results delineated an approximately triangular-shaped potential sliding body within the soil.

ACKNOWLEDGEMENTS

The study is funded by National Key R&D Program of China (No. 2023YFC3007001).

REFERENCES

Hu, W.D., Hu, T., Lin, S.C., Tang, J.G., Zhou, Y.B., Hu, Q.S. (2024). Experimental study on deformation and passive earth pressure behind cantilever pile retaining walls in narrow excavations. *Geotechnical and Geological Engineering*, 42: 7041-7061. https://doi.org/10.1007/s10706-024-02912-3

Liu, C., Yan, C.D., Zheng, G., Liu, T., Yang, Y.H. (2023). Field testing and numerical analysis of supporting performance of oblique piles used in pit excavation. *International Journal of Geomechanics*, 23(11): 04023204. https://doi.org/10.1061/IJGNAI.GMENG-8487

Zhang, Q., Hu, J., Wang, J., He, P., Hou, L.L., Lin, P., Song, S.G. (2021). Study on the mechanical behavior of a foundation pit retaining structure adjacent to the pile foundation of a subway station. *Environmental Earth Sciences*, 80: 704. https://doi.org/10.1007/s12665-021-09996-7

Li, Y.J., Zhou, Z.W., Alcalá, J., Yepes,V. (2025). Research on spatial deformation monitoring and numerical coupling of deep foundation pit in soft soil. *Journal of Building Engineering*, 99: 111636. https://doi.org/10.1016/j.jobe.2024.111636

Ren, B.K., Shen, Y., Zhao, T.T., Li, X.J. (2023). Deformation monitoring and remote analysis of ultra-deep underground space excavation. *Underground Space*, 8: 30-44. https://doi.org/10.1016/j.undsp.2022.04.005

Liu, J.W., Shi, C.H., Cao, C.Y., Lei, M.F., Wang, Z.X. (2020). Improved analytical method for pile response due to foundation pit excavation. *Computers and Geotechnics*, 123: 103609. https://doi.org/10.1016/j.compgeo.2020.103609

Wang, Z., Guo, B.L., Wei, G., Hu, C.B., Zhang, L.S. (2023). Simplified deformation analyses of a single pile subjected to different deformation modes of the pit enclosure structure. *International Journal of Geomechanics*, 23(4): 04023014. https://doi.org/10.1061/IJGNAI.GMENG-8019

Bai, J.G., Li, H.J. (2024). Numerical simulation study on steel pipe row pile support of temporary road slope. *Jordan Journal of Mechanical and Industrial engineering*, 16(5): 743-752. https://jjmie.hu.edu.jo/vol16-5/08-JJMIE-194-22

Chi, Z., Deng, M. (2024). Progressive failure mechanism of existing-supplementary double-layer piles retaining excavation beneath existing underground space. *Scientific Reports*, 14: 24357. https://doi.org/10.1038/s41598-024-75987-w

Song, Y., Li, S.Q., Lou, G.C., Hao, G., Meng, S.Y., Liu, C. (2025). Research on Selection Parameters of Isolation-Support Dual-Purpose Piles Based on Orthogonal Tests. *Advance in Civil Engineering*, 1: 7420194. https://doi.org/10.1155/adce/7420194

Zhang, G., Hu, Y., Zhang, J.M. (2009). New image analysis-based displacement-measurement system for geotechnical centrifuge modeling tests. *Measurement*, 42(1): 87-96. https://doi.org/10.1016/j.measurement.2008.04.002

Zhang, G., Yan, G.C. (2016). In-flight simulation of the excavation of foundation pit in centrifuge model tests. *Geotechnical Testing Journal*, 39(1): 59-68. https://doi.org/10.1520/GTJ20150028